Drop-Size Distributions from Pneumatic Atomizers

K. Y. KIM and W. R. MARSHALL, JR.

University of Wisconsin, Madison, Wisconsin

A study was made of the atomizing characteristics of convergent-type pneumatic nozzles. Drop-size correlations were obtained for the following ranges: drop size, 6 to 350 μ, mass median diameter; mass flow ratio, 0.06 to 40; relative velocity, 250 ft./sec. to sonic velocity; and viscosity. 1 to 50 cp. The technique employed was to spray cool a molten wax, and melts of wax-polyethylene mixtures. The most important operating variables in pneumatic atomization are the dynamic force of the atomizing gas, and the mass flow ratio of air to liquid. The cumulative volume drop-size distribution of spray from a pneumatic nozzle was fitted by a modified logistic equation. Empirical correlations developed in the study can be used to design nozzles or to predict drop size for sprays produced by the types of nozzles studied. In particular, this study provides new experimental data on the performance of pneumatic atomizers in producing relatively large drops.

Pneumatic atomization is a process of producing sprays by the disruptive action of a high-velocity gas upon a liquid jet. Because two fluid streams are involved, it is sometimes called two-fluid atomization. Pneumatic nozzles are particularly well-suited to produce fine sprays, that is, less than 50 μ in mass median diameter. Other methods of atomization, such as pressure nozzles and spinning disks, are not generally capable of producing sprays of this drop-size range except under extreme operating conditions. However, the fine-size production from pneumatic atomizers is accomplished only with relatively modest capacities, several gallons per hour at most. Nevertheless, this type of atomization has an advantage in that liquid and air streams can be controlled independently. Some viscous fluids and thick suspensions can be atomized by pneumatic nozzles better than pressure nozzles.

A knowledge of the drop-size distribution in sprays from pneumatic nozzles permits predictions of the performance of equipment using such sprays. However, drop-size data from pneumatic nozzles are scarce. The objectives of this study were to investigate a wide range of drop-size distributions and to obtain a correlation for convergent-type nozzles. The size range studied was about sixtyfold, 6 to 350 μ for the mass median diameter.

SOME PREVIOUS WORK

Pneumatic atomization has attracted the attention of a number of investigators (*2* to *4*, *8* to *12*, *14* to *16*, *19*, *21*, *27*, *28*). However, the published drop-size distribution data for these atomizers are fragmentary and not well related. Even when a correlation is available, it is only applicable to the specific nozzle designs over the ranges of the variables studied. The range of variables for several other investigators has been summarized (Table A), and is available elsewhere.*

A drop-size correlation by Nukiyama and Tanasawa (*19*) probably has been the most widely quoted work in pneumatic atomization.

$$\bar{x}_{vs} = \frac{585}{v_{rel}}\sqrt{\frac{\sigma}{\rho_l}} + 597\left(\frac{\mu_l}{\sqrt{\rho_l\sigma}}\right)^{0.45}(1000\,Q_a/Q_l)^{1.5} \tag{1}$$

Analysis of Equation (1) of Nukiyama and Tanasawa shows that for ratios of Q_a/Q_l greater than 5,000, the second term has slight influence on drop size; the size is determined by relative velocity and liquid properties (except viscosity). Nozzle dimensions do not enter the correlation.

The average* drop size from a pneumatic nozzle decreases with increase of air-to-liquid ratio (*2*, *4*, *9*, *9a*, *11*, *12*, *16*, *19*, *21*, *28*). This fact appears to be a consistent observation of all investigators, even though the degree or extent of its effect is varied. An additional finding has been that the increase in relative velocity decreases drop size (*19*, *27*, *28*). The effect of nozzle dimensions reported by various workers, however, appears to be contradictory. Thus Gretzinger (*12*) reported a drop-size decrease; Nukiyama and Tanasawa (*19*), no effect; Wetzel (*27*) and Wigg (*28*), a drop-size increase with increase of liquid nozzle diameter.

Most investigations to date suggest that the drop sizes from pneumatic nozzles are primarily a function of liquid rate, gas rate, atomizing gas pressure, nozzle diameters, flow ratio, and viscosity. The atomizing gas pressure is not especially fundamental in evaluating the performance of an atomizer, since the gas velocity and density can better express atomization pressure.

Assuming that the drop size from pneumatic nozzles is affected by gas and liquid nozzle diameters, gas turbulence parameter T (having a dimension of length), fluid densities, fluid viscosities, liquid surface tension, relative velocity, and flow rates, one can combine these factors into dimensionless groups.

$$\frac{\bar{x}}{T} = f\left(\frac{D_a}{D_l}, \frac{D_l v^2_{rel}\rho_a}{\sigma}, \frac{M_a}{M_l}, \frac{\mu_l}{\sqrt{D_l\rho_l\sigma}}, \frac{\mu_l}{\mu_a}, \frac{\rho_l}{\rho_a}\right) \tag{2}$$

The dimensionless groups on the right-hand side are ratio of diameter of gas and liquid nozzles (defining nozzle design), Weber number (dynamic and surface tension forces), mass flow ratio (feed conditions), Z number

K. Y. Kim is at Monsanto Company, St. Louis, Missouri.

* Tables A to D and Figures A to C have been deposited as document 01321 with the ASIS National Auxiliary Publications Service, c/o CCM Information Sciences, Inc., 909 Third Ave., New York 10022 and may be obtained for $2.00 for microfiche or $6.50 for photocopies.

* No specific type of average is referred to here.

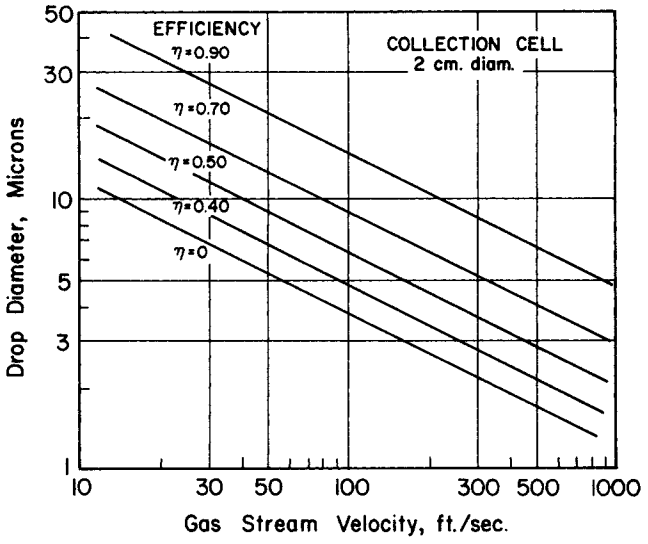

Fig. 1. Collection efficiency of an immersion cell estimated from Ranz' work.

(viscosity force), and viscosity and density ratios. These are the usual groups encountered in atomization.

ATOMIZATION STUDY TECHNIQUES

Drop-size evaluations of atomizers require the collection of a representative sample from a spray in flight. This may be achieved by a variety of techniques, such as collection in an immersion cell containing immiscible liquids (*1, 12, 18, 24, 25*). However, many factors must be considered critically in any sampling techniques. Collection efficiency and evaporation are two of the most important of such factors.

If an immersion cell is placed in a flowing aerosol or spray, streamlines will be set up around the cell. Large drops have enough inertia to impact on the surface, but small drops tend to follow the streamlines. The collection efficiency can be estimated from the work of Ranz and Wong (*22*). For collection by inertial impaction, they expressed collection efficiency as a function of the inertial size parameter, defined as

$$\Psi = \rho_l v x^2 / 18\, \mu_g\, D_c \qquad (3)$$

For the case of an aerosol stream of infinite extent, computed results for a 2-cm. collection cell are shown in Figure 1. Diameters at zero efficiency are considered to be the minimum sizes which can be collected at a specified stream velocity. For example, drops smaller than 4.0 μ cannot be expected to be collected in an air stream at 100 ft./sec. velocity. It is therefore concluded that sampling with an immersion cell or any other impingement collector is not reliable for sprays below 50 μ, unless the stream velocity is extremely high, probably in excess of 1,000 ft./sec.

The lifetime of a small drop is short. The evaporation time of a pure liquid drop at low or zero Reynolds number is given by (*7*)

$$\theta = \lambda\, \rho_l x_0^2 / 8\, k\, \Delta t \qquad (4)$$

The lifetime of water droplets may be calculated from Equation (4). For instance, a 10-μ drop has a lifetime of about 1 sec. in a 90% relative humidity atmosphere. This estimation was substantiated by Gretzinger (*12*), who observed that water droplets of 15 to 20 μ which had been collected in oil disappeared completely in seconds. Consiglio and Sliepcevich (*6*) reported that they could not collect drops below 13 μ in low humidity surroundings.

Since the drop sizes from pneumatic atomizers are usually small, evaporation effects are of considerable significance, and hence the representativeness of the sample collected can be in serious question. Thus the drop-size data from pneumatic atomizers based on direct drop collection methods tend to be larger than actual sizes. To avoid these undesirable effects, Gretzinger (*12*) employed a spray drying method which involved the size analysis of spray-dried particles and the conversion of the data to original liquid spray drop size by means of a material balance on the solids in the liquid drops and dry particles. This method is practical only when the density of the spray-dried particles is known. However, spray-dried products are usually hollow, and the particle density is a complex function of particle size and drying conditions. Therefore its applicability is practical only for a small size range where dry solid particles are obtained.

One method of overcoming this disadvantage is to spray a liquid which will solidify in the surrounding atmosphere. For example, Joyce (*14*) used a paraffin wax to simulate the physical properties of fuel oil. The same technique was used by others (*9*), (*21*). Wetzel (*27*) studied venturi atomization by using a low melting point alloy. Turner and Moulton (*26*) sprayed benzoic acid and beta-naphthol.

The spray cooling technique was used in this study. A microcrystalline wax was atomized and the total spray was frozen and collected. A representative sample for size determination was taken from the entire mass of particles.

EXPERIMENTAL PROCEDURES

Atomizers

A convergent, external mixing-type pneumatic atomizer was investigated in this study. Atomizing gas converged and expanded through an annulus around a liquid nozzle. The air mixed with liquid outside the atomizer.

A versatile atomizer was designed consisting of five major parts: nozzle fastener, air nozzle, main body, liquid nozzle, and

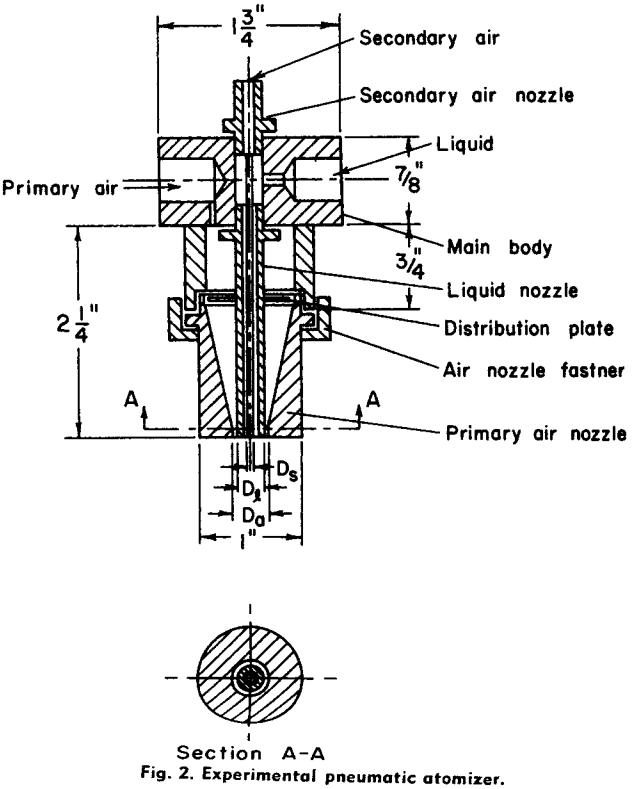

Fig. 2. Experimental pneumatic atomizer.

Table 1. Details of the Pneumatic Atomizers Studied

1. Dimensions of nozzles

Symbol	Air nozzle Diam. (D_a), in.	Area, sq. in.	Liquid nozzle Symbol	O.D. (D_l), in.	I.D., in.	Area for liquid, sq. in.
A-1	0.1285	0.01131	L-1	0.072	0.054	0.002290
A-2	0.166	0.02164	L-2	0.125	0.105	0.008659
A-3	0.272	0.05811	L-3	0.250	0.222	0.03871
S.S.N.†	0.120	0.01297	S.S.N.†	0.100	0.060	0.00283

2. Area and clearance of air annulus with various combinations

Insert series	I		II		III	
Nozzle combination	A-1 L-1		A-2 L-2	A-3 L-3	A-2 L-1	A-3 L-1	A-3 L-2
Clearance, in.	0.0283		0.0205	0.011	0.047	0.100	0.0735
Area, sq. in.	0.00890		0.00937	0.00902	0.0176	0.0540	0.0458

3. Dimensions of concentric double air nozzle atomizer

Primary air nozzle diam., in.	Secondary air nozzle O.D., in.	Secondary air nozzle I.D. (D_s), in.	Liquid nozzle O.D., in.	Liquid nozzle I.D., in.	Areas of flow Primary air, sq. in.	Areas of flow Secondary air, sq. in.	Areas of flow Liquid sq. in.
0.272	0.095	0.073	0.250	0.222	0.00902	0.00418	0.0316

† Fluid nozzle 60100, air nozzle 120, Spraying Systems Company.

secondary air nozzle (Figure 2). The first four parts were assembled to give an atomizer with a single gas nozzle, and all five parts an atomizer with two gas nozzles. In the latter arrangement, the secondary gas nozzle was inserted axially in the liquid nozzle. Thus an annular liquid sheet was produced between two air streams. Three sets of air and liquid nozzles were fabricated. They were designed so that the atomizer formed could have the same air flow area. The nozzle dimensions and flow areas of atomizers formed with the various combinations of air and liquid nozzles are presented in Table 1. A Spraying Systems Company pneumatic nozzle (¼)J was also studied.

Liquids

The liquids atomized were molten wax and melts of wax-polyethylene mixtures of various composition to obtain variations in viscosity. The wax was Crown 1035, a microcrystalline, branched hydrocarbon mixture. It had an average molecular weight of 890 and a melting point of 195° to 200°F. (*27*). The polyethylene used was Epolene N with an average molecular weight of 2,500. It had a softening point of 223°F.

The melt density, viscosity, and surface tension were experimentally determined for wax-polyethylene mixtures. The melt viscosity was correlated by a Flory-type equation (*15*). All atomization runs were made at 230°F., liquid temperature. The physical properties at this temperature are summarized in Table 2. All the melts atomized in this study were Newtonian fluids.

Solidified wax particles were mostly spherical are shown in Figure 3. Some of the particles appeared to have been formed by coalescence. Coarse particles larger than 30μ had always one or several air bubbles. Average void volume percent was measured to be 1.8% of the particle volume.

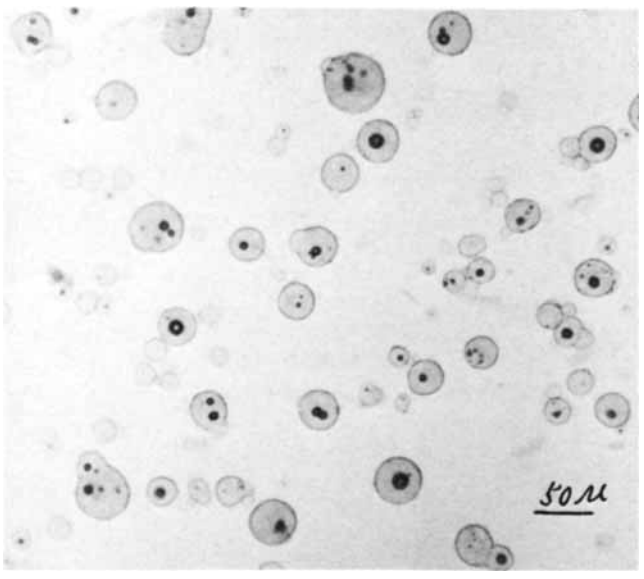

Fig. 3. Photomicrograph of wax particles.

Equipment

A schematic diagram of the experimental setup used in spray cooling runs is given in Figure 4. The wax or wax-polyethylene mixture was melted in a steam-jacketed reservoir. Liquid flow was produced by air pressure, and the flow rate was controlled by a needle valve. Atomization was carried out with hot air at the melt temperature. The wax was atomized into a cylindrical opening which led to a chamber measuring 3 ft. × 8 ft. × 4 ft. The atomizing air was pumped out by a blower through a cloth filter. The wax spray was solidified in the chamber and settled on the floor of the chamber. After atomization, an opening in the top of the chamber was opened to induce downward air current in order to accelerate particle settling. After the chamber became clear, the solidified spray particles on the floor were collected intact. Usually 97% of the input was collected.

Size Analysis

Particle size was determined by two techniques: microscope counting and sieving. The borderline size for sieving was approximately 70μ, mass median diameter. The total mass of col-

Table 2. Physical Properties of Wax-Polyethylene Mixtures at 110°C.

Composition	Viscosity, cp.	Density, g./cc.	Surface tension, dynes/cm.
Wax	8.70	0.834	29.6
Wax and 10% Epolene N	24.0	0.782	31.2
Wax and 20% Epolene N	49.2	0.782	31.2

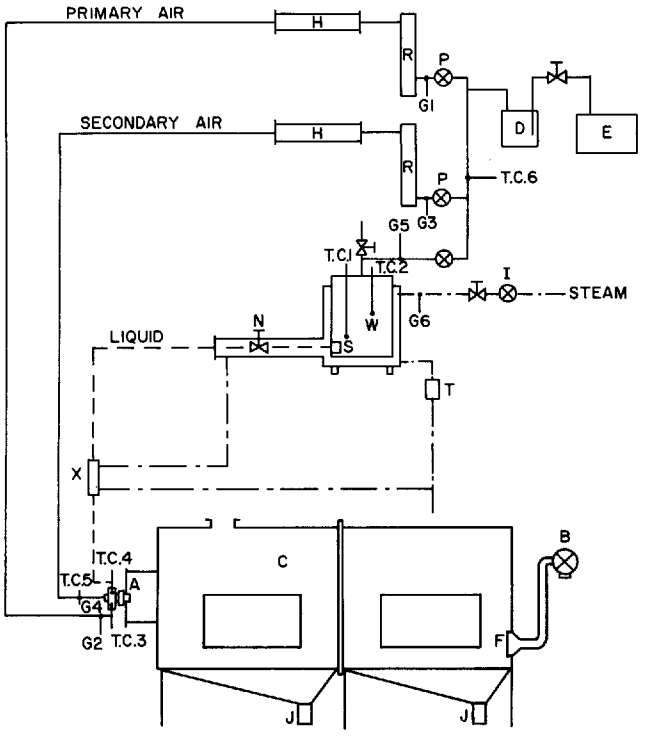

Fig. 4. Schematic diagram of the experimental setup used in spray cooling.

lected particles was mixed well and the sample size was reduced by a quartering process. Reproducible sieving results were obtained within 15 min. About 1,000 particles were counted by the microscope technique. Since frequencies of coarse particles were small compared with finer ones, and yet their contribution to the volume distribution was large, an additional 300 to 500 larger particles were counted. The distributions were then combined using the ratio of coarse to fine particles obtained in the general counting. Figure 5 shows the analyses of a sample using the two techniques. The data points for each method can be connected with a single curve.

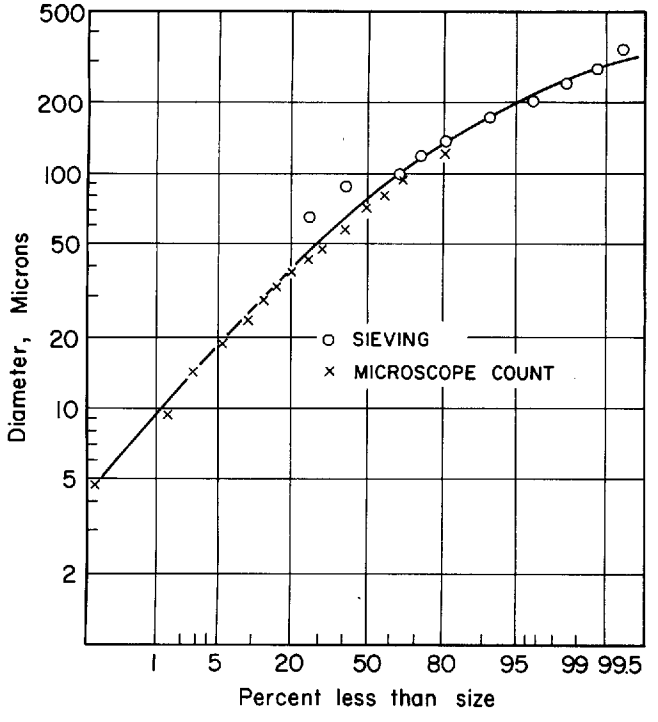

Fig. 5. Comparison of distributions obtained by the different analytical techniques.

Calculation

The linear velocity of atomizing gas at the nozzle in the subsonic region was calculated from

$$v = Q/A = 4Q/\pi\,(D_a^2 - D_l^2) \tag{5}$$

The sonic or acoustic velocity was calculated from

$$a = \sqrt{g_c\,\kappa RT/M_w} \tag{6}$$

For air at 230°F. the acoustic velocity is 1,287 ft./sec. Relative air velocity was obtained by subtracting the liquid velocity from the gas velocity. For most runs the liquid velocity was negligible compared with the gas velocity. The gas density at the air nozzle in the sonic range was estimated from the measured mass flow rate as follows:

$$\rho_a = G/v_a = M_a/v_a A \tag{7}$$

In the subsonic region the gas density of 0.0576 lb./cu.ft. at 230°F. was used.

Microscope sizing method produces number frequency data. It was found that number distribution data obtained in this study could not be fitted by any of the usual distribution functions. Therefore the number frequency data of a sample were processed by a digital computer to calculate number, surface, and volume frequencies, together with the following statistical averages:

$$\phi_{ni} = n_i/\Sigma n_i \tag{8}$$

$$\phi_{si} = \phi_{ni}\,x_i^2/\Sigma\phi_{ni}\,x_i^2 \tag{9}$$

$$\phi_{vi} = \phi_{ni}\,x_i^3/\Sigma\phi_{ni}\,x_i^3 \tag{10}$$

volume mean diameter $$x_v = (\Sigma\phi_{ni}\,x_i^3)^{1/3} \tag{11}$$

Sauter mean diameter $$x_{vs} = \Sigma\phi_{ni}\,x_i^3/\Sigma\phi_{ni}\,x_i^2 \tag{12}$$

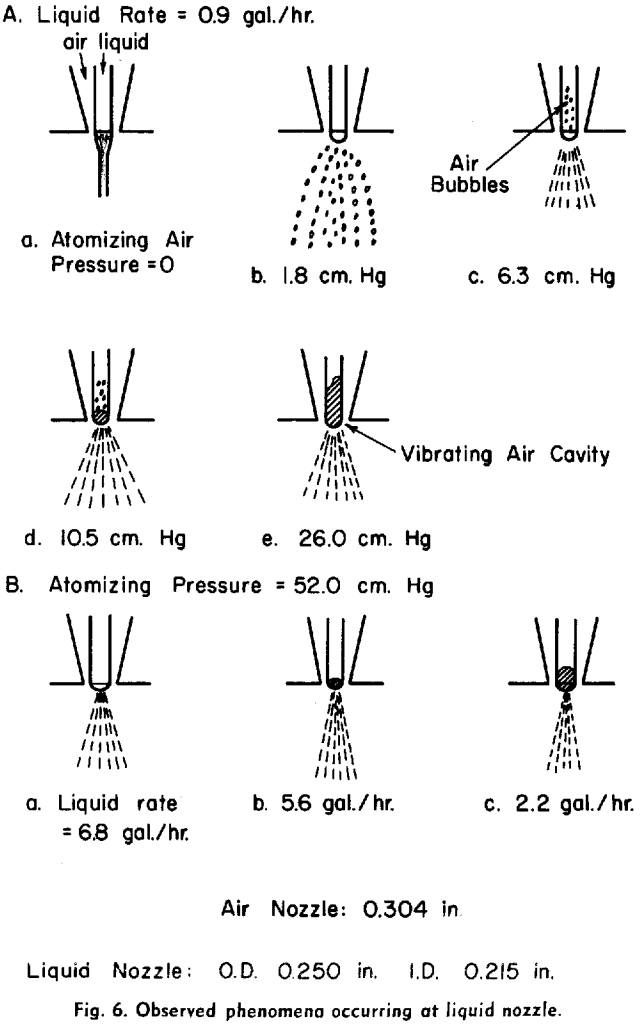

Fig. 6. Observed phenomena occurring at liquid nozzle.

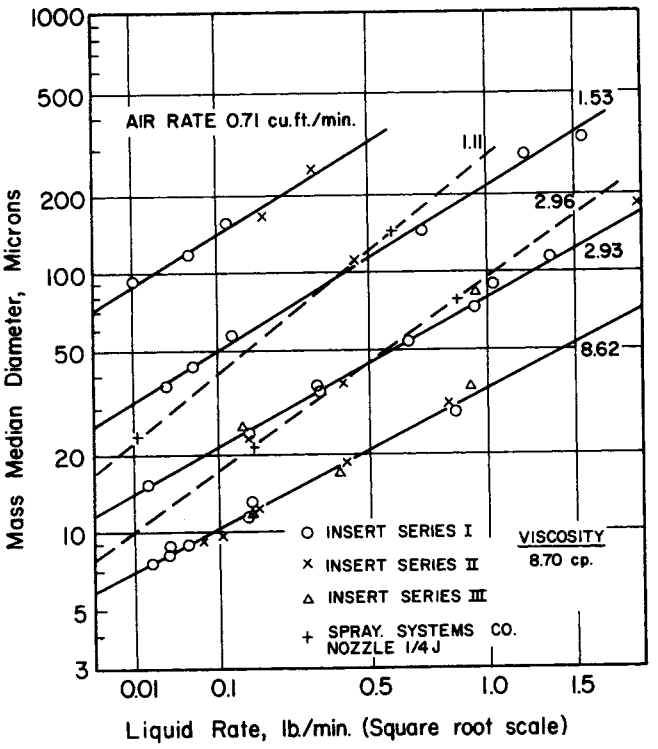

Fig. 7. Effect of liquid rate on spray drop size (convergent type and low viscosity).

For x_i^2 and x_i^3 in the above equations, the surface-weighted mean and volume-weighted mean, respectively, of the i^{th} class were used assuming a uniform distribution within the class. For instance, the surface-weighted mean was calculated as follows:

$$(\overline{x_s^2})_i = \int_{I_{(i-1)}}^{I_i} x^2 dx \Big/ \int_{I_{(i-1)}}^{I_i} dx \qquad (13)$$

EXPERIMENTAL RESULTS

Phenomena Occurring at Liquid Nozzle

The behavior of the fluids issuing from the nozzles was visually observed using Lucite atomizers. Sketches of the observed phenomena are presented in Figure 6. At low air flow rate the liquid jet formed a conical tip before breakup. As the air pressure increased, the tip surface became wavy and air bubbles appeared in the liquid. In the next stage, an air cavity started to form near the edge of the nozzle. The invaded portion of the liquid nozzle became a zone of turbulent swirling air. Further increase in air pressure caused a deeper and more turbulent air cavity in the liquid nozzle. Liquid lamellae under the influence of air cavity vibration crept to the liquid nozzle edge and disintegrated. The air vibration appeared to be one of the causes for the pulsations in pneumatic atomization. This observation discouraged correlating drop size in terms of calculated film thickness at the nozzle.

Drop-Size Data

Volume distribution data from the computer was interpolated to obtain the volume median diameter. Since the wax particles were practically solid, this median was directly proportional to the mass median diameter $\overline{x}_m$, which was used for correlation of results.

A plot of logarithm of $\overline{x}_m$ versus the square root of liquid mass flow rate was found to be linear for a given nozzle and air rate, as shown in Figure 7. The slopes of these lines increased as the air rate decreased. The slope also varied with nozzle design.

Figure 8 shows the effect of air-to-liquid mass ratio on the mass median diameter for a range of values of $v_{rel}^2 \rho_a$ (corresponding to a certain air rate). A study of the several families of curves as shown in Figure 8 revealed the following trends.

1. The mass median diameter of a spray decreased and approached a limiting mass median diameter for each air rate as the ratio M_a/M_l increased. At small values of M_a/M_l, all the curves converged. At a ratio of 0.1, the spray deteriorated.
2. The mass median diameter of a spray at a constant M_a/M_l was larger for lower air velocities for a given atomizer; that is, at low air velocities the air dynamic force is low.
3. A family of curves shifted as the nozzle design of an atomizer changed.
4. The increase of the liquid viscosity shifted a family of curves (for a nozzle) upward (coarse) with little change in shape.

It was indicated that the mass median diameter approached an asymptote for a given air nozzle. This is the limiting diameter which can be obtained as $M_a/M_l \to \infty$. The limiting mass median diameters are given in Table 3 as determined by extrapolating the plots of log $\overline{x}_m$ versus

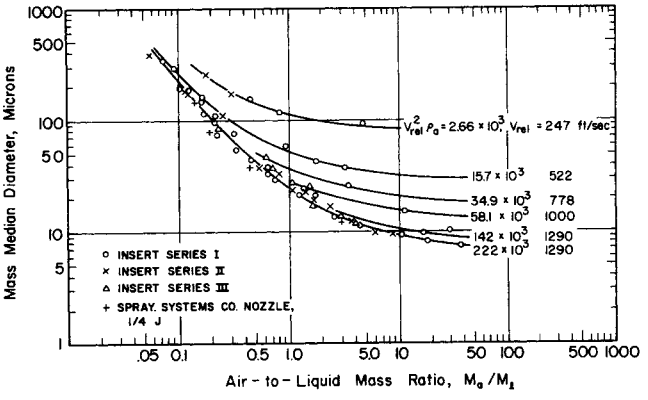

Fig. 8. Effect of mass ratio on spray drop size (convergent type and low viscosity range). V_{rel}, ft./sec.; ρ_a, lb./cu. ft.; viscosity, 8.70 cp.

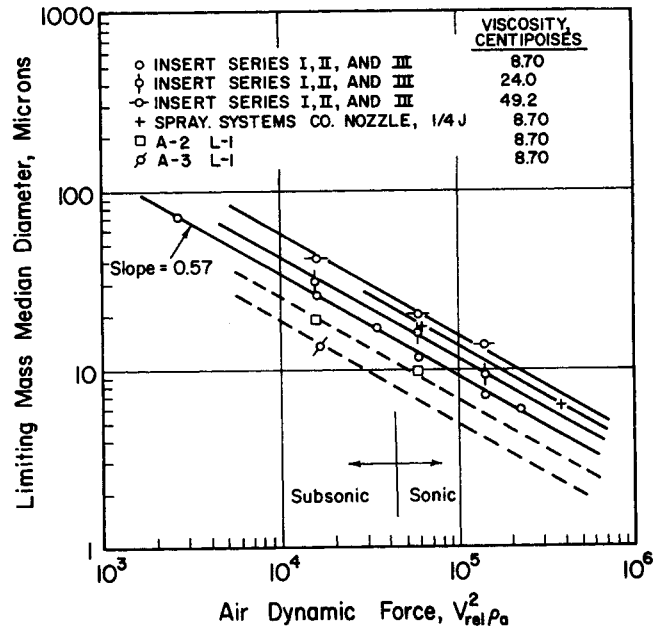

Fig. 9. Correlation of limiting mass median diameter as a function of dynamic force of air.

$\sqrt{M_l}$ using the least square method. The limiting mass median diameter was found to be a function of the dynamic force of atomizing gas (Figure 9), viscosity (Figure 10), and total air rate. The lines in Figure 9 are parallel. Their locations depend upon nozzle combination and viscosity. The average slope −0.57 may be applicable generally to convergent-type atomizers. For atomizers of different design, presumably lines of different slope would be obtained because of differences in the mode of air-liquid interaction. The limiting mass median diameter decreased with the 0.36 power of the atomizing air rate. The variation in total air rate at constant air velocity and air density was produced by changes in the air nozzle cross-sectional area.

Drop-size data were obtained with 10% (24.0 cp.) and 20% (49.2 cp.) mixtures of Epolene N with the wax. Since the surface tension and density were practically constant, the change in drop size was considered to be caused by the change in liquid viscosity. With high viscosity liquids, the effect of liquid rate on the mass median diameter was similar to that shown in Figure 7 but with steeper slopes. For a given M_a/M_l and $v_{rel}^2\rho_a$ high viscosity liquids yielded coarser sprays.

The insert series I and II (Table 1) gave practically identical performances for the whole range of the variables. The insert series III (with the largest liquid nozzle), however, had a tendency to produce coarser sprays, especially at low air-to-liquid ratios. There seems to be three distinct regions in which the liquid nozzle diameter affects the drop size of a spray. The Weber number, $N_{We} = D_l v_{rel}^2 \rho/\sigma$, is useful in defining the regions. In the first region an issuing liquid jet is solid when it meets air (Figure 6A, *b*, and *c*). Therefore the increase of liquid jet diameter results in a coarser spray as reported by Wetzel (*27*) due to lack of efficient interaction. For an intermediate region, probably corresponding to Figure 6A, *d*, in which the liquid jet begins to cavitate at the nozzle tip, the liquid nozzle diameter would affect the drop size negligibly. Further increase of N_{We} causes the air to invade the liquid nozzle (Figure 6A, *e*), causing the liquid to issue in the form of a film. In this region the drop size probably decreases with the increase of liquid contact perimeter as reported by Gretzinger (*12*).

The concentric characteristic of the air and liquid nozzle

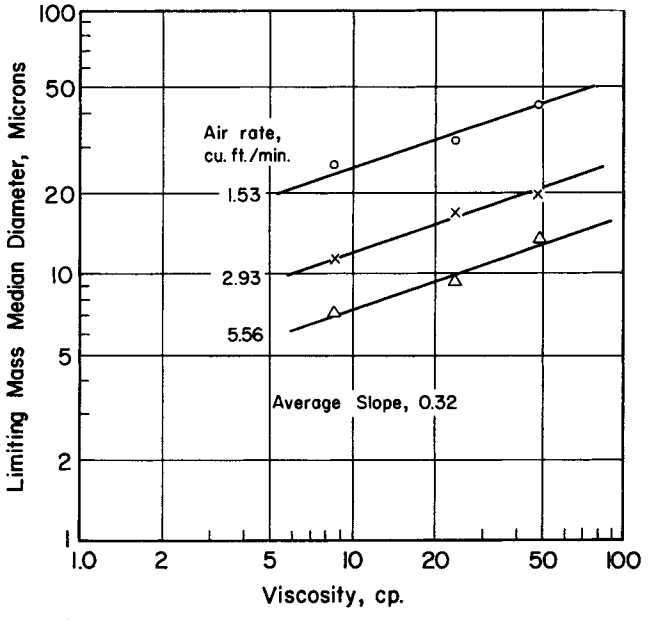

Fig. 10. Correlation of limiting mass median diameter as a function of liquid viscosity.

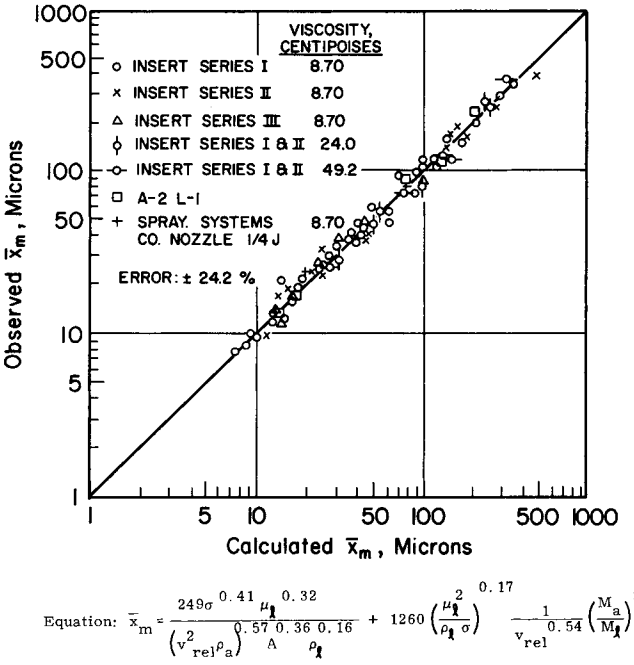

Equation: $\bar{x}_m = \frac{249\sigma^{0.41}\mu_l^{0.32}}{(v_{rel}^2\rho_a)^{0.57} A^{0.36} \rho_l^{0.16}} + 1260\left(\frac{\mu_l^2}{\rho_l\sigma}\right)^{0.17} \frac{1}{v_{rel}^{0.54}}\left(\frac{M_a}{M_l}\right)^m$

Fig. 11. Correlation for convergent-type pneumatic atomizer.

is an important factor in obtaining fine and reproducible sprays. Any eccentricity resulted in coarser and more nonuniform sprays. The effect was prominent at low air-to-liquid ratios, but became less pronounced at higher mass ratios.

Correlations

Correlations of the effects of air velocity, liquid rate, viscosity, density, etc., led to the following empirical equation for the atomizer with a single air nozzle.

$$\bar{x}_m = 249 \frac{\sigma^{0.41}\mu_l^{0.32}}{(v_{rel}^2\rho_a)^{0.57} A^{0.36} \rho_l^{0.16}} + 1260\left(\frac{\mu_l^2}{\rho_l\sigma}\right)^{0.17} \frac{1}{v_{rel}^{0.54}}\left(\frac{M_a}{M_l}\right)^m \quad (14)$$

where $m = -1$, if $M_a/M_l < 3$; $m = -0.5$, if $M_a/M_l > 3$.

Figure 11 shows a plot of observed log $\bar{x}_m$ versus calculated log $\bar{x}_m$ by Equation (14). The error range is ± 24.2% at 95% confidence level.

For the concentric double air nozzle atomizer, a similar treatment of drop-size data as for the convergent type was made, and the mass median diameter of a spray was correlated by an analogous equation:

$$\bar{x}_m = \frac{8140}{(v_{rel}^2\rho_a)_{av}^{0.72}}\left[\frac{\sigma^{0.41}\mu_l^{0.32}}{\rho_l^{0.16}}\right] + 1240\left(\frac{\mu_l}{\rho_l\sigma}\right)^{0.17} \frac{1}{(v_a)_{av}^{0.54}}\left(\frac{M_a}{M_l}\right)^m \quad (15)$$

where $m = -1$, if $M_a/M_l < 3$; $m = -0.5$, if $M_a/M_l > 3$.

$$v_{av} = f(v_{rel})_{pri} + (1-f)(v_{rel})_{sec} \quad (16)$$

f = weight fraction of total air flowing in primary nozzle

$$(v_{rel}^2\rho_a)_{av} = f(v_{rel}^2\rho_a)_{pri} + (1-f)(v_{rel}^2\rho_a)_{sec} \quad (17)$$

It is interesting to note that the exponent of dynamic force, $v_{rel}^2\rho_a$, is 0.72 instead of 0.57, suggesting a different mode of air-liquid interaction resulting from the different design. The total air throughput in the atomizer was still the predominant factor in determining drop size. Fig-

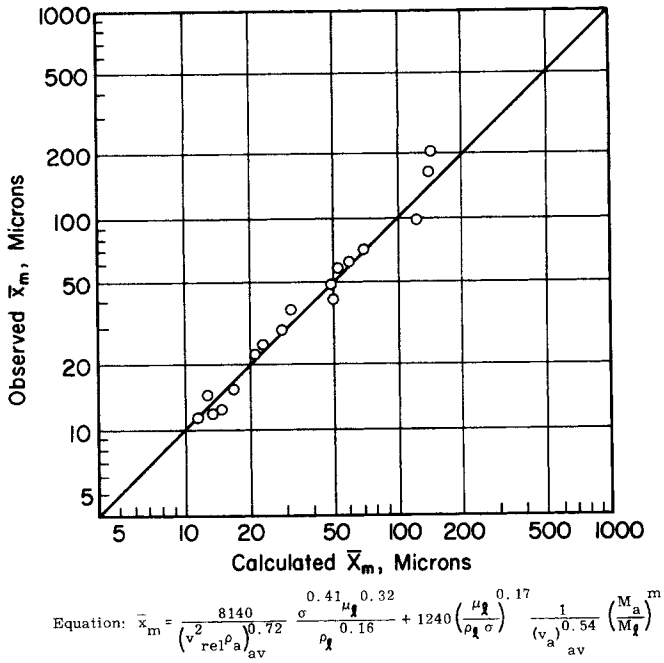

Fig. 12. Concentric double air nozzle atomizer correlation.

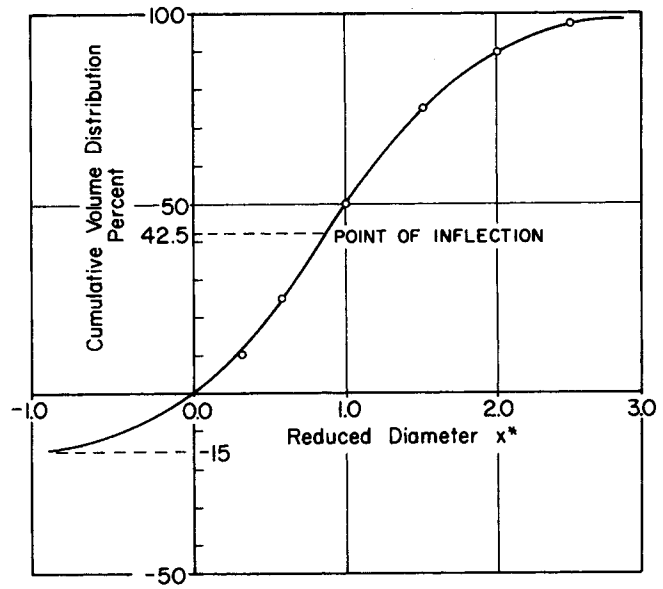

Fig. 13. Generalized volume distribution from convergent-type pneumatic atomizers.

ure 12 is a comparison of observed drop size with drop size calculated from Equation (15).

Drop-Size Distributions

Neither the number nor the calculated volume distributions followed the usual distribution functions such as logarithmic, square root probability (*17*, 25), or Rosin-Rammler (23).

When the distribution data of sprays having nearly the same mass median diameter but produced by widely different operating conditions were plotted, all data points of cumulative volume distribution between 10 and 90% sizes fell on a single curve. For the convergent-type atomizers, various percentage diameters were found to be linearly proportional to the median diameter (Table B).*

A generalized cumulative distribution of particle volume (or mass) was obtained by plotting the proportionality constant for a corresponding percentage diameter against a reduced diameter, $x^* = \bar{x}/x_m$, as shown in Figure 13. The generalized distribution curve had an inflection point at approximately 42.5% diameter. If the curve was extended smoothly to the range of negative diameter, it became symmetrical about the inflection point. This suggested fitting the curve by a Pearl-Reed or logistic equation (*20*).

$$\Phi_v - b = \frac{b(1-b)}{b - \exp(a\,r\,x)} \tag{18}$$

Figure 14 shows the curve fitting by this equation. The constants b and r were found graphically to be -0.150 and -2.18, respectively. When we substitute $1/\bar{x}_m$ for the constant a, Equation (18) becomes

$$\Phi_v = \frac{1.15}{1 + 6.67 \exp(-2.18x^*)} - 0.150 \tag{19}$$

This equation has an inflection point at $\Phi_v = 0.42$ and $x^* = 0.87$. By differentiating Equation (19) with respect to x^*, one gets the volume frequency function as

$$\phi_v = \frac{16.7 \exp(-2.18x^*)}{[1 + 6.67 \exp(-2.18x^*)]^2} \tag{20}$$

Surface and number distribution functions can also be derived by appropriate multiplying factors. Number, surface, and volume distribution data from both microscope counting and sieve analyses were found to satisfy these equations very well. Figure 15 shows the fitting of data from a screen analysis by Equations (19) and (20).

The Sauter mean diameter was found to be proportional to mass median distribution as follows:

$$\bar{x}_{vs} = 0.83 \cdot \bar{x}_m \tag{21}$$

Thus the Sauter mean diameter can be estimated from Equation (21) in conjunction with Equation (14).

The concentric double air nozzle atomizer produced

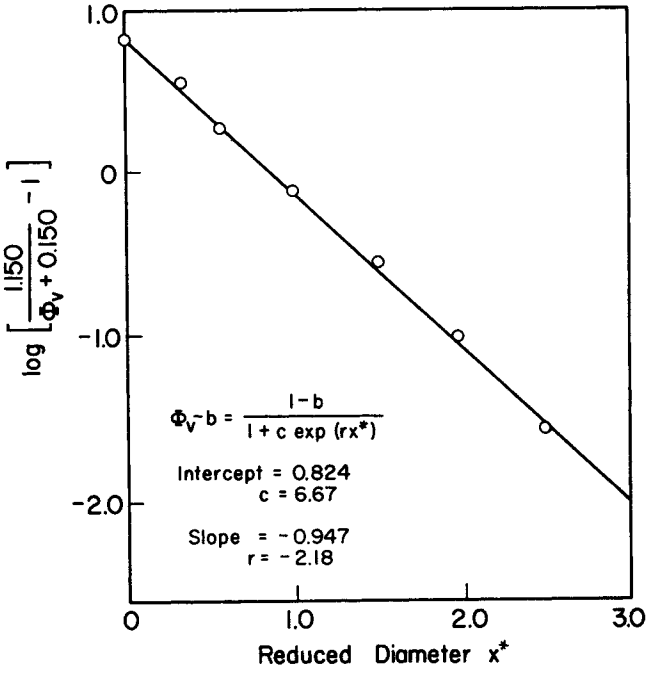

Fig. 14. Generalized volume distribution curve fitted by the logistic equation.

* See footnote on p. 575.

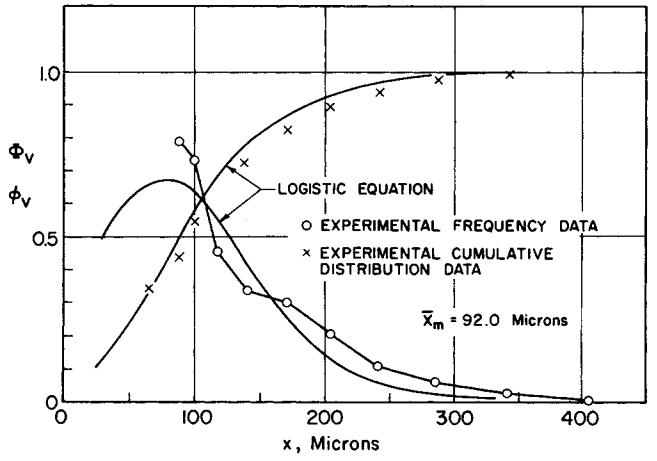

Fig. 15. Screen analysis data fitted by the logistic equation.

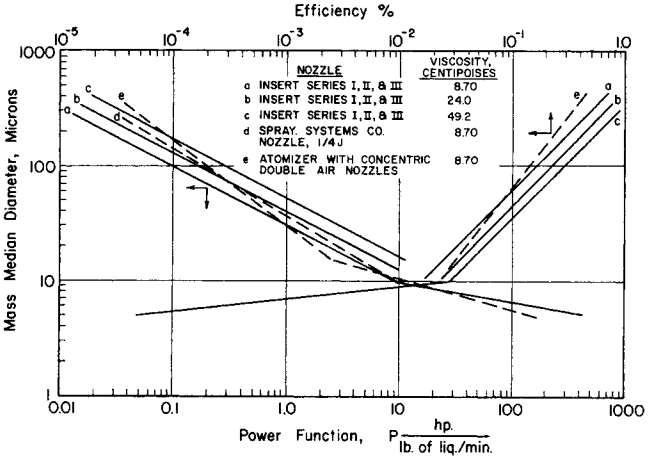

Fig. 16. Variation of spray drop size with power function and efficiencies of pneumatic atomizers.

drop-size distributions quite different from those of the convergent type. For a given median diameter, the double air stream atomizer produced more uniform sprays for larger drop sizes, 40 μ, but less uniform sprays for smaller sizes than the convergent atomizers.

Power Requirements and Efficiency

The power consumed by the nozzles in this study was calculated based on isothermal expansion of the air using the following equation:

$$P = \frac{1}{M_w} \cdot \frac{M_a}{M_l} RT \ln \frac{p}{p_e} \tag{22}$$

The calculated power consumption was correlated with mass median diameter, Figure 16. In general, the mass median diameter was expressed by an equation of the following type:

$$x_m = c\, P^n \tag{23}$$

The parameters c and n were found to be a function of atomizer design; c also increased as viscosity increased. It was found that there was a critical value of mass median diameter, about 10 μ, at which an abrupt change in n took place. This suggested that an abrupt increase in the resistance to breakup had developed at this particular drop size. Thus the exponent on the power changed from -0.5 to -0.12 at a mass median diameter of 10 μ.

The efficiency of atomization, defined as the ratio of energy to create new surface to the actual energy used, is given by

$$\eta = \frac{P_t/M_l}{P} = \frac{6\sigma}{\rho\, \bar{x}_{vs}\, P} \tag{24}$$

Using the $\bar{x}_{vs}$ versus $\bar{x}_m$ relationship, Equation (21), the efficiency was expressed as a function of $\bar{x}_m$ and plotted in Figure 16.

The efficiency of an atomizer was found to be proportional to $\bar{x}_m$ or some power of $\bar{x}_m$, depending on nozzle design. Around 10 μ the efficiency decreased abruptly. For coarse sprays, such as 100 μ in mass median diameter, the efficiency was about a few tenths of a percent and comparable to other methods of atomization (*17*). However, for very fine sprays of 5 μ, mass median diameter, the efficiency was extremely low, 10^{-4}%.

DISCUSSION

Drop-Size Correlation Compared with Other Results

The drop-size correlation expressed by Equation (14) has a form similar to the Nukiyama and Tanasawa equation, Equation (1). However, the latter equation predicts larger drop sizes than Equation (14), especially for similar conditions, and in the smaller size range. Equation (1) was determined from data obtained by a physical sampling technique which probably was liable to nonrepresentative samples because of the evaporation and target effects discussed earlier. Gretzinger's data (*12*) correlated well with Equation (14) if 3,100 is used for the second-term coefficient instead of 1,260. Wetzel's drop-size data for venturi atomization (*27*) were correlated with an equation similar to Equation (14). However, the correlation equation for his data had different coefficients and powers from those of this investigation, which is believed to be a reflection of differences in nozzle design. The drop sizes predicted by the correlation of this study agreed well with those determined by the spray drying technique employed by Gretzinger (*12*). (Refer to Table C).*

Modified Logistic Equation as Size-Distribution Function

Spray size distributions from pneumatic atomizers investigated by Gretzinger (*12*) and Wetzel (*27*) also fitted well with Equation (19) and the same set of constants (see Figure A).* It is remarkable, if not fortuitous, that one set of constants in Equation (19) can predict the size distribution of sprays from pneumatic atomizers of different dimensions and design features.

Limiting Mass Median Diameter and Taylor's Theory

Taylor (*25a*) studied the instability of a viscous liquid interacting with a high-velocity air stream. Most probable wavelengths in terms of the dimensionless group, $\lambda_m \rho_a v^2/2\pi\sigma$, were expressed as a function of a viscosity parameter, $(\rho_l/\rho_a)\,\sigma^2/\mu_l^2 v^2$. The two limiting cases are noted (see Figure B).*

1. if $\left(\frac{\rho_l}{\rho_a}\right)\left(\frac{\sigma^2}{\mu_l^2 v^2}\right) < 10^{-3}$,

$$\frac{\lambda_m\, \rho_a\, v^2}{2\pi\sigma} = \frac{4\rho_a\, \mu_l^2\, v^2}{3\rho_l\, \sigma^2} \tag{25}$$

(high viscosity)

2. if $\left(\frac{\rho_l}{\rho_a}\right)\left(\frac{\sigma^2}{\mu_l^2 v^2}\right) > 10^3$, $\frac{\lambda_m\, \rho_a\, v^2}{2\pi\sigma} = \frac{3}{2}$ (26)

(low viscosity)

* See footnote on page 575.

TABLE 3. LIMITING MASS MEDIAN DIAMETER
(Convergent Type)

Nozzle	Viscosity, cp.	Air rate, cu. ft./min.	Relative velocity, ft./sec.	Limiting mass median diameter, μ
Insert series I	8.70	0.710	247	71.4
	8.70	1.53	522	25.2
	8.70	2.28	778	16.8
	8.70	2.93	1,000	11.4
	8.70	5.56	1,290 (sonic)	7.15
	8.70	8.67	1,290	5.83
Insert series II	24.0	1.53	522	31.2
	24.0	2.93	1,000	16.6
	24.0	5.56	1,290	9.12
Insert series III	49.2	1.53	522	42.3
	49.2	2.93	1,000	19.8
	49.2	5.56	1,290	13.4
S.S.N.	8.70	1.11	900	17.0
	8.70	2.56	1,290	10.5
	8.70	5.60	1,290	6.10
A-2 L-1	8.70	2.98	512	18.7
A-2 L-1	8.70	5.75	988	9.80
A-3 L-1	8.70	4.46	250	41.0
A-3 L-1	8.70	9.38	531	13.5
A-3 L-2	8.70	7.88	537	14.5

If it is assumed that a statistical drop-size diameter is proportional to the most probable wavelength, the wavelength would indicate the order of the average drop diameter of a spray. The proportionality constant appears to be around unity if Equation (26) is compared with Hinze's survival diameter (*13a*) expressed as a critical Weber number, for shock exposure, and for

$$N_{vi} = \mu_l/\sqrt{x\,\sigma\,\rho_l} = 0$$

$$N_{We\ crit} = \frac{x v^2 \rho_a}{\sigma} \approx 13 \qquad (27)$$

Most probable wavelengths predicted by Taylor's theory were compared with the limiting mass median distribution (Table 3) experimentally determined in this study (see Table D for comparisons).† Interestingly, the most probable wavelength came to ± 50% of the observed limiting mass median diameter.

If the above-mentioned hypothesis is acceptable, it can be further seen that the drop size would be proportional to $v^{-4/3}$ from Equation (25) at low values of the viscosity parameter (high liquid viscosity) and to v^{-2} from Equation (26) at the higher value of the parameter (low viscosity). This study showed that the limiting size is proportional to $v^{-1.14}$ and $v^{-1.44}$ (double air nozzle).

From Taylor's analysis, the effect of liquid viscosity on drop size can be predicted. He gave a correction factor, which is to be applied to the wavelength calculated from Equation (26), versus the viscosity group $\mu_l/\sqrt{\rho_l\,\sigma\,\lambda_m}$. (See Figure C.)* The range of the viscosity group in this investigation was approximately 0.2 to 1.5. A straight line in this region of the graph has an estimated slope of 0.37, which is close to the viscosity exponent of 0.32 determined from the current wax data.

The wave theory suggests an explanation for the variation of the limiting drop size produced from a pneumatic nozzle. However this theory is not applicable for explaining all aspects of the pneumatic atomization process. There are undoubtedly several simultaneous mechanisms involved when a jet is atomized by the forces and interaction of a high-velocity gas stream. The task of experimentally evaluating and relating these mechanisms remains difficult indeed.

SOME OBSERVATIONS AND CONCLUSIONS

This study has presented drop-size correlations which can be used to predict the mass median diameters of sprays produced by pneumatic atomizers. The correlations are specific to the nozzle designs studied and to Newtonian fluids. However, the correlation may be useful with modifications of coefficients and/or powers of variables for other nozzle designs.

This study has verified over a wide range of conditions that the important operating variables in pneumatic atomization are the air-to-liquid mass ratio and the dynamic force of atomizing air. Increasing either the mass ratio or the air dynamic force, or both, decreases the drop size of the sprays. The drop size in the coarse sprays depends largely upon the mass ratio, while the effect of the dynamic force predominates in the finer range. As Newtonian viscosity increases, sprays become coarser. In general, a given mean spray size formed with a pneumatic atomizer can be expressed as follows:

$$x = \frac{a}{(v_{rel}^2 \rho_a)^\alpha} + b\left(\frac{M_a}{M_l}\right)^\beta \qquad (28)$$

The exponents α and β are functions of nozzle design and a and b, those of both nozzle design and liquid properties.

When an atomizer is operated at very large mass ratios, the mass median drop size of a spray approaches an asymptote, which is a function of air dynamic force and liquid properties. This was regarded as the limiting mean size in this study. It characterizes the finest spray obtainable with a specific atomizer and air input. The most important operating variables which affected the limiting mass median diameter were found to be gas velocity and density at the gas-liquid interaction point.

The recommended operating range of the mass ratio is about 0.1 to 10. Below the lower limit atomization deteriorates, and above the upper limit atomization is done with excess energy expenditure.

The atomizer with concentric double air nozzles had nearly the same performance as the convergent type within the ranges studied. The uniformity of the sprays formed with this type is a little better than for sprays with the single air nozzle.

A modified logistic equation was used to characterize the drop-size distribution from a convergent-type atomizer. Good fitting of other investigators' data with this type of equation indicated that it may have general usefulness for describing the characteristics of distributions from convergent-type pneumatic nozzles.

ACKNOWLEDGMENT

The authors acknowledge the assistance and helpfulness of the Wisconsin Alumni Research Foundation, the University of Wisconsin Numerical Analysis Laboratory, and the Engineering Experiment Station.

NOTATION

A = area, sq.ft.; also flow area for atomizing air, sq.in.
a = acoustic velocity, ft./sec.; also a constant in a logistic equation
b = lower asymptote in a logistic curve; also a con-

* See footnote on p. 575.

stant
c = constant
D_a, D_l = diameters of air and liquid nozzles, respectively, in.
D_c = diameter of an immersion cell, cm.
D_s = diameter of secondary air nozzle, in.
f = weight fraction of air flowing in the primary air nozzle in the concentric double air nozzle atomizer
G = mass velocity, lb./(sq.ft.)(sec.)
g_c = gravitational constant
I = class intervals, μ
k = thermal conductivity
M_a, M_l = mass flow rate of atomizing air and liquid, respectively, lb./min.
M_w = molecular weight
m = constant, exponent of air-to-liquid mass ratio
N = total number of drops
N_{We} = Weber number, $D_l v^2 \rho_a/\sigma$
n = constant, exponent of power function
P = power, hp./lb. of liquid
P_t = theoretical power requirement for producing new surface
p = absolute atomizing pressure, lb./sq.in.
p_e = ambient pressure into which a liquid is atomized
Q_a, Q_l = volumetric flow rates of air and liquid, respectively
Q = cu.ft./min.
R = gas constant
r = parameter in a logistic equation
T = absolute temperature; also gas turbulence parameter
t = temperature gradient
v = velocity of gas stream, ft./sec.
v_a, v_l = linear velocities of air and liquid, respectively, at nozzle, ft./sec.
v_{rel} = relative velocity, $v_a - v_l$, ft./sec.
x = drop diameter, μ
x_0 = initial diameter of a drop, μ
x^* = reduced diameter, $x/\bar{x}_m$
x_{10}, x_{25}, x_{75}, x_{90} = diameters corresponding to the respective percents in cumulative volume distribution, μ
$\bar{x}$ = general notation for a mean of a drop-size distribution, μ
$\bar{x}_m$ = mass median diameter, μ
$(\bar{x}_m)_0$ = limiting mass median diameter, μ
$\bar{x}_s$ = surface mean diameter, μ
$\bar{x}_v$ = volume mean diameter, μ
$\bar{x}_{vs}$ = Sauter mean or volume-to-surface mean diameter, μ

Greek Letters

α = constant, exponent of mass ratio
β = constant, exponent of dynamic force
η = collection efficiency of an immersion cell in sample collection or efficiency of energy expenditure in the formation of new surface
ρ_a, ρ_l = air and liquid densities, respectively, lb./cu.ft., in Equation (1), g./ml.
σ = surface tension, dynes/cm.
κ = specific heat ratio
θ = drop lifetime, sec.
μ_a, μ_l, μ_g = viscosities of air, liquid, and gas, respectively, cp.
λ = latent heat of vaporization; also wavelength
Φ_n, Φ_s, Φ_v = relative cumulative distributions less than, referring to number, surface, and volume, respectively
ϕ_n, ϕ_s, ϕ_v = relative frequency referring to number, surface, and volume, respectively.
Ψ = inertial size parameter for impaction of drops on a target

Subscripts

a = air
calc = calculated
g = gas
i = i^{th} size class
l = liquid
m = mass, or most probable
n = number
o = initial or limiting
ob = observed
pri = primary
rel = relative
s = surface
sec = secondary
v = volume

LITERATURE CITED

1. Adler, C. R., and W. R. Marshall Jr., *Chem. Eng. Progr.*, **47**, 515 (1951).
2. Anson, D., *Fuel*, **32**, 39 (1953).
3. Bitron, M. D., *Ind. Eng. Chem.*, **47**, 23 (1955).
4. Burton, E. J., and J. R. Joyce, *J. Inst. Fuel*, **30**, 395 (1957).
5. Cambel, A. B., and B. H. Jennings, "Gas Dynamics," p. 47, McGraw-Hill, New York (1958).
6. Consiglio, J. A., and C. M. Sliepcevich, *AIChE J.*, **3**, 418 (1957).
7. Duffie, J. A., and W. R. Marshall, Jr., *Chem. Eng. Progr.*, **49**, 417, 480 (1953).
8. Edeling, C., *Beihefte Angew. Chem.*, **57**, 56 (1950).
9. Fraser, R. P., "Proceedings of 2nd Industrial Conference," Fermhurst Res. Sta., London, England (1957).

9a. ———, N. Dombrowski, and J. H. Routley, *Chem. Eng. Sci.*, **18**, 339 (1963).

10. Garner, F. H., and V. E. Henny, *Fuel*, **32**, 151 (1953).
11. Golitzine, N., C. R. Sharp, and L. G. Badham, *Natl. Aeronaut. Estab. Canada, R-14, ME-186*, Ottawa (1951).
12. Gretzinger, J., and W. R. Marshall, Jr., *AIChE J.*, **7**, 312 (1961).
13. Herring, W. M., Jr., and W. R. Marshall, Jr., *ibid*, **1**, 200 (1955).

13a. Hinze J. O., *ibid.*, **1**, 289 (1955).

14. Joyce, F. R., *J. Am. Soc. Naval Eng.*, **61**, 659 (1949).
15. Kim, K. Y., Ph.D. thesis, Univ. Wisconsin, Madison (1959).
16. Lewis, H. C., et al., *Ind. Eng. Chem.*, **40**, 67 (1948).
17. Marshall, W. R., Jr. *Chem. Eng. Progr. Monogr. Ser.* No. 2 (1954).
18. McIrvine, J. D., Ph.D. thesis, Univ. Wisconsin, Madison (1957).
19. Nukiyama, S., and Y. Tanasawa, *Trans. Soc. Mech. Eng. Japan, 4-6 Rept. 1-6* (1938-40).
20. Pearl, R., "Medical Biometry and Statistics," p. 417, 2nd ed., W. B. Saunders Co., Philadelphia (1930).
21. Radcliffe, A., and H. Clare, *Rept. No. R. 144*, Natl. Gas Turb. Establishment, England (1953).
22. Ranz, W. E., and J. B. Wong, *Ind. Eng. Chem.*, **44**, 1371 (1952).

22a. Ranz, W. E., *Bull. No. 65*, Pennsylvania State Univ. Dept. Eng. Res. (Mar. 26, 1956).

23. Rosin, P., and J. Rammler, *J. Inst. Fuel*, **7**, 29 (1933).
24. Rupe, J. H., "Third Symposium on Combustion, Flame and Explosion Phenomena," pp. 680-94, Williams and Wilkins, Baltimore (1949).
25. Tate, R. W., and W. R. Marshall, Jr., *Chem. Eng. Progr.*, **49**, 169, 226 (1953).
26. Turner, G. M., and R. W. Moulton, *ibid.*, **49**, 185 (1953).
27. Wetzel, H., Ph.D. thesis, Univ. Wisconsin, Madison (1951).
28. Wigg, L. D., *J. Inst. Fuel*, **37**, 500 (1964).

Manuscript received May 3, 1967; revision received March 2, 1970; paper accepted March 2, 1970.